Roadmaps Incorporating Respiratory and Cardiac Motion for X-ray Fused with MRI

A. Z. Faranesh[1], P. Kellman[1], and R. J. Lederman[1]
[1]Division of Intramural Research, National Heart Lung and Blood Institute, National Institutes of Health, Bethesda, Maryland, United States

Introduction: X-ray fused with MRI (XFM) integrates anatomic and functional information from MRI with x-ray angiography, providing enhanced image guidance for interventional procedures [1]. The MRI derived roadmaps serve to increase procedure efficacy and reduce radiation dosage [2]. To increase the fidelity of the roadmaps so that they accurately reflect physiological motion, respiratory and cardiac motion need to be incorporated. Previous work has explored using a global affine model to represent respiratory motion [3], but such a model is valid for a single cardiac phase, and does not allow for regional differences in motion within the heart. In this work, respiratory and cardiac motion measured from real-time MRI images are combined in a composite affine model used to resolve physiologic motion in MRI roadmaps overlaid on live x-ray fluoroscopy.

Methods: Imaging studies were performed on anesthetized swine. All procedures were approved by the Institutional Animal Care and Use Committee. Real-time MRI images were acquired on a 1.5T Espree scanner (Siemens Medical Solutions, Erlangen, Germany) under free breathing (respirator), with ECG surface electrode recording. Multiple planes (e.g. coronal, sagittal and three-chamber views) were acquired so that the superior surface of the diaphragm and heart were in the field of view. A SSFP sequence was used with TR/TE =2.8/1.4ms; FOV=360x270mm; matrix=192x92; TSENSE acceleration factor=2; acquisition time=30s. As described previously [4], a respiratory navigation signal was automatically derived from the images and, together with the ECG signal, was used to sort the images according to respiratory and cardiac phase. The images were interpolated to a grid in the respiratory cardiac plane. For each plane, contours were drawn on an image at end-expiration, end-diastole, for the epicardium, endocardium and right ventricle. These ROIs were propagated over all respiratory and cardiac phases using non-rigid registration [5]. Once the 3D contours for all respiratory and cardiac phases were determined, they were fit to affine models. To compute the affine transforms, cardiac motion and respiratory motion were analyzed independently. For each respiratory phase r, the cardiac affine transform $\mathbf{C}(r,c)$ was computed, which maps motion from end-diastole (ED) to cardiac phase c. For each cardiac phase c, the affine transform $\mathbf{R}(r,c)$ was computed, which maps motion from end expiration (EE) to respiratory phase r. The affine transforms were computed by solving the least squares problem $\mathbf{Ax}=\mathbf{y}$, where $\mathbf{A}$ is the affine transformation, $\mathbf{x}$ is the set of 3D points at EE or ED, and $\mathbf{y}$ is the set of 3D points at some cardiac-respiratory phase. The affine transforms were computed separately for each individual anatomic contour. To generate the roadmap, ECG-gated breath-hold SSFP cine images were acquired in multiple 2D slices to cover the heart from base to apex. The respiratory phase was automatically detected from an image-based navigator on the x-ray image, and the ECG signal was recorded to determine cardiac phase. To transform contour $\mathbf{x}(EE,ED)$ from end-diastole, end-expiration, to $\mathbf{x}(r,c)$ at point (r,c) in the cardiac-respiratory plane, the affine transforms were applied serially: $\mathbf{R}(r,c)\mathbf{C}(EE,c)\mathbf{x}(EE,ED)=\mathbf{x}(r,c)$.

Results: The diaphragm was successfully tracked from the MRI real-time images, providing a respiratory navigation waveform, as shown in Fig. 1. The RMS error between the affine model fit contours and manually drawn contours was less than 3mm over all contours and respiratory-cardiac phases. The elements of the affine matrices corresponded well with expected physiological motion (Fig. 2). The diaphragm was successfully tracked in the x-ray angiography images, and the affine deformed roadmap tracked well with the heart shadow in x-ray angiography (Fig. 3).

Conclusion: We have implemented a method for incorporating cardiac and respiratory motion into MRI derived roadmaps fused onto live xray angiography. The use of individual affine models for different anatomic structures accommodates complex physiological motion while maintaining computational efficiency. The resulting enhanced roadmap should improve the efficacy of XFM guided procedures.

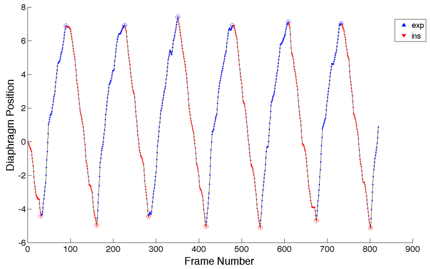

Figure 1: Respiratory navigator waveform from tracking the diaphragm position on real-time MRI images. Blue=expiration; red=inspiration.

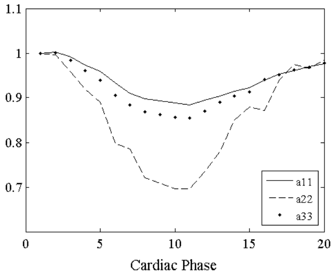

Figure 2: Diagonal elements of affine transform representing scaling of endocardial surface over cardiac cycle.

References: 1. Gutierrez LF, Med Phys. 2008; 2. Ratnayaka K, JACC Cardiovasc Interv. 2009; 3. King AP, Med Image Anal. 2009; 4. Kellman P, Magn Reson Med. 2008; 5. Chefd'hotel C Proc ISBI. 2002.

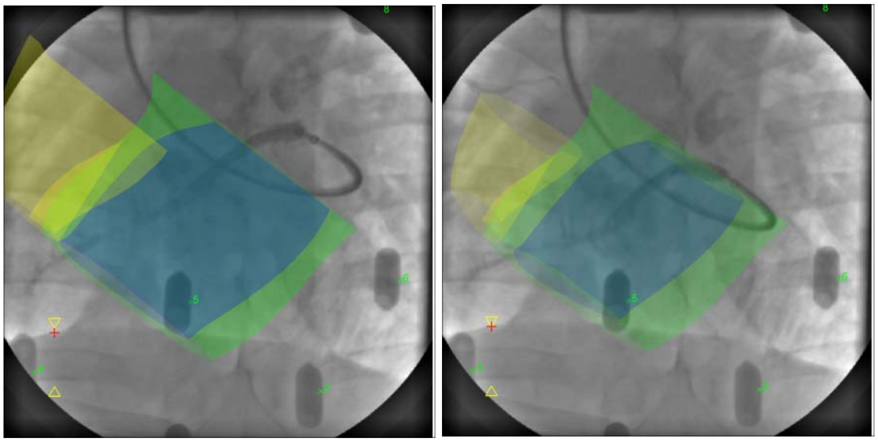

Figure 3: MRI-derived roadmaps overlaid on x-ray angiographic images. Diastolic (left) and systolic (right) phases are shown. Green=left ventricle epicardium; blue=left ventricle endocardium; yellow=right ventricle endocardium. The image-based navigator (red plus sign) is shown on the lower-left of the images.